IJFANS International Journal of Food and Nutritional Sciences

ISSN PRINT 2319 1775 Online 2320 7876

Research paper **UGC CARE Listed (Group -I) Journal Volume 10, Spl Iss 1, 2021**

Improving Plate-Type Heat Exchanger Thermal Performance with Alumina-Titania Hybrid Suspensions: An In-Depth Performance Evaluation

Atul Bhattad, Koneru Lakshmaiah Education Foundation (KLEF), Vaddeswaram 522302, Andhra Pradesh, India

Abstract

This paper discusses the development of models for predicting the thermal conductivity and viscosity of hybrid nanofluids composed of both aluminum oxide (Al2O3) and titanium dioxide (TiO2) nanoparticles. The investigation focuses on how varying the fluid temperature (ranging from 283 K to 298 K) affects the performance of a plate heat exchanger utilizing Al2O3-TiO2 hybrid nanofluids with different particle volume ratios (0:5, 1:4, 2:3, 3:2, 4:1, and 5:0). These nanofluids are prepared with a 0.1% concentration in deionized water. Experimental assessments are conducted to evaluate several key parameters, including heat transfer rate, Nusselt number, heat transfer coefficient, Prandtl number, pressure drop, and performance index. The study findings reveal noteworthy trends. As the TiO2 ratio increases, there is a decrease in the heat transfer coefficient, Nusselt number, and heat transfer rate. This decline can be attributed to the lower thermal conductivity of TiO2 in comparison to Al2O3. Conversely, an increase in the inlet temperature leads to a decrease in pressure drop and the performance index. Remarkably, the Al2O3 (5:0) nanofluid demonstrates the most significant enhancement, with improvements of approximately 16.9% in the heat transfer coefficient, Nusselt number, heat transfer rate, and performance index. On the other hand, the TiO2 (0:5) hybrid nanofluid exhibits modest enhancements of 0.61% and 2.3% for pressure drop and Prandtl number, respectively.

1. Introduction

Heat exchangers encounter several heat transfer issues during fluid flows. For this reason, industries have adopted the addition of nanoparticles to the working fluid to improve heat exchanger performance. Additives have been considered to enhance thermal properties [1]. Nanofluids are colloidal mixtures of base fluids and nano-sized particles (10–100 nm) [2]. Combining nanoparticles with base fluids makes it possible to improve thermal conductivity, density, viscosity, and specific heat, leading to enhanced heat transfer. Nanofluids can be synthesised in a single or two-step process. Due to their enhanced thermal conductivity, nanofluids find wide applications in various fields, such as heat exchangers, solar energy, refrigeration systems, and thermo-siphons. The thermal conductivity of nanofluids can be measured using the 3-! method, temperature oscillation, and transient hot-wire techniques. The constants in models or empirical relationships utilised to evaluate nanofluids' thermal conductivity and viscosity are based on experimental data[3].

2. Preparation and Characterization of Hybrid Nanofluids

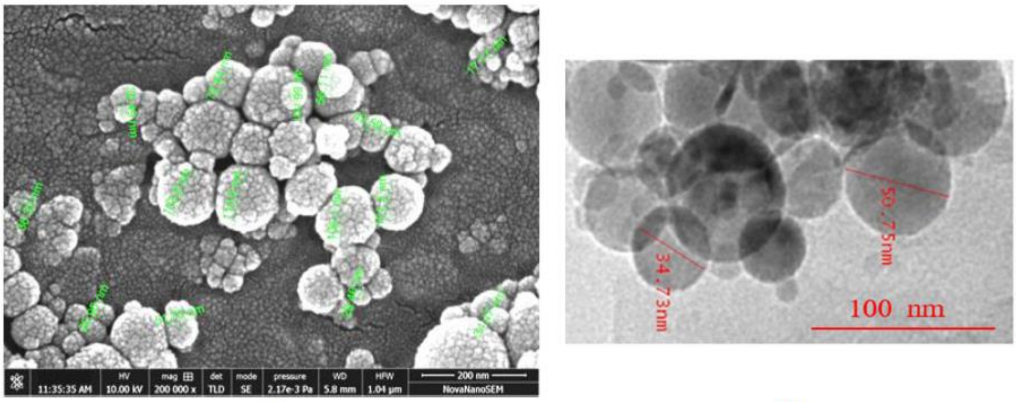

(a) (b)

Figure 1. (a). SEM image of Al_2O_3- TiO_2/water hybrid nanofluid; (b). TEM image of Al_2O_3-TiO_2/water hybrid nanofluid.

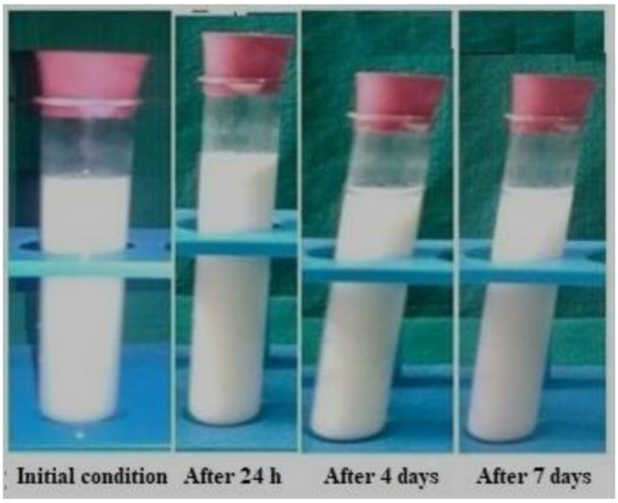

Figure 2. Stability analysis of a sample showing no sedimentation for 7 days.

Figure 3. Hot disk thermal constants analyser.

Figure 4. Brookfield digital viscometer.

3. Performance of PHE with Hybrid Nanofluid

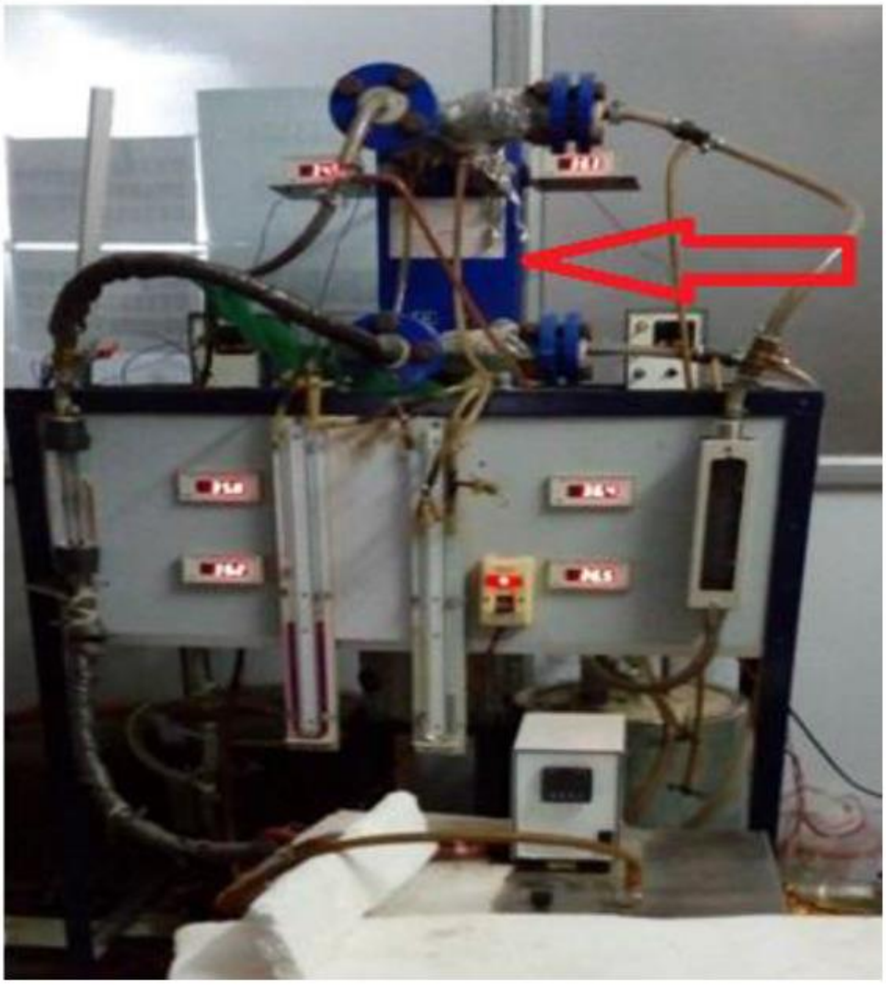

Figure 5. Experimental setup showing PHE with a red arrow.

Table 1. (a). Thermo-physical properties of DI water. (b). Thermo-physical properties of hybrid nanofluids.

(a)					
T (K)	k_{bf} (W/m-K)	ρ_{bf} (kg/m^3)	μ_{bf} (mPa·S)	C_{Pbf} (J/kg·K)	Pr_{bf}
283	0.5823	997.8	0.9549	4183	6.774
288	0.5896	996.8	0.8706	4183	6.106
293	0.5964	996.0	0.8150	4183	5.668
298	0.6014	994.7	0.7493	4183	5.157

Table 1. *Cont.*

(b)						
T (K)	Al_2O_3–TiO_2–WaterNanofluids					
	TiO_2(0:5)	Hybrid (1:4)	Hybrid (2:3)	Hybrid (3:2)	Hybrid (4:1)	Al_2O_3(5:0)
Thermal Conductivity, k_{hnf} (W/m-K)						
283	0.5919	0.5921	0.5921	0.5921	0.5922	0.5922
288	0.5979	0.5993	0.5993	0.5994	0.5994	0.5994
293	0.6036	0.6046	0.6046	0.6047	0.6047	0.6047
298	0.6091	0.6100	0.6101	0.6109	0.6109	0.6109
Density, ρ_{hnf} (kg/m^3)						
283	1001.0	1000.9	1000.9	1000.8	1000.8	1000.7
288	1000.0	999.7	999.7	999.6	999.6	999.5
293	999.0	998.8	998.7	998.7	998.7	998.6
298	997.9	997.7	997.6	997.4	997.4	997.3
Viscosity, μ_{hnf} (mPa·S)						
283	0.9684	0.9684	0.9684	0.9684	0.9684	0.9684
288	0.8935	0.8786	0.8786	0.8786	0.8786	0.8786
293	0.8275	0.8187	0.8187	0.8187	0.8187	0.8187
298	0.7690	0.7612	0.7612	0.7535	0.7535	0.7535
Specific Heat, Cp_{hnf} (J/kg·K)						
283	4169	4169	4169	4169	4169	4169
288	4169	4169	4169	4169	4169	4170
293	4169	4169	4169	4169	4169	4170
298	4168	4169	4169	4169	4169	4170
Prandtl Number, Pr_{hnf}						
283	6821	6819	6819	6819	6817	6817
288	6230	6112	6112	6111	6111	6112
293	5715	5645	5645	5644	5644	5646
298	5262	5202	5202	5142	5142	5143

Table 2. Thermal conductivity for Al_2O_3 and TiO_2 nanofluids (0.1 v%) with temperature.

T (K)	Thermal Conductivity (W/m·K)					
	Al_2O_3 Nanofluid			TiO_2 Nanofluid		
	Test	$f_k = 4.4$ in Equation (10)	$f_k = 8.8$ in Equation (10)	Test	$f_k = 4.4$ in Equation (10)	$f_k = 8.8$ in Equation (10)
283	0.5922	0.5840	0.5858	0.5919	0.5836	0.5850
288	0.5994	0.5917	0.5939	0.5979	0.5912	0.5929
293	0.6047	0.5990	0.6016	0.6029	0.5983	0.6003
298	0.6109	0.6045	0.6077	0.6089	0.6038	0.6061

Table 3. Thermal conductivity data of Al_2O_3 nanofluid at 323 K for different concentrations.

Concentration (ϕ)	Thermal Conductivity (W/m·K)		Concentration (ϕ)	Thermal Conductivity (W/m·K)	
	Test [56]	$f_k = 8.8$ in Equation (10)		Test [56]	$f_k = 8.8$ in Equation (10)
0.005	0.6884	0.6953	0.035	0.8400	0.8408
0.010	0.7232	0.7276	0.040	0.8590	0.8593
0.015	0.7484	0.7546	0.045	0.8779	0.8771
0.020	0.7737	0.7787	0.050	0.8969	0.8942
0.025	0.7990	0.8007	0.055	0.9127	0.9107
0.030	0.8179	0.8213	0.060	0.9285	0.9268

Table 4. Thermal conductivity of hybrid nanofluids at different temperatures and particle ratio.

Fluid	Temperature, T (K)			
	283	288	293	298
DI Water	0.5896	0.5964	0.6014	0.6077
TiO_2 (0:5)	0.5919	0.5979	0.6029	0.6089
Hybrid (1:4)	0.5920	0.5983	0.6031	0.6094
Hybrid (2:3)	0.5921	0.5985	0.6035	0.6098
Hybrid (3:2)	0.5921	0.5987	0.6039	0.6102
Hybrid (4:1)	0.5922	0.5992	0.6043	0.6106
Al_2O_3 (5:0)	0.5922	0.5994	0.6047	0.6109

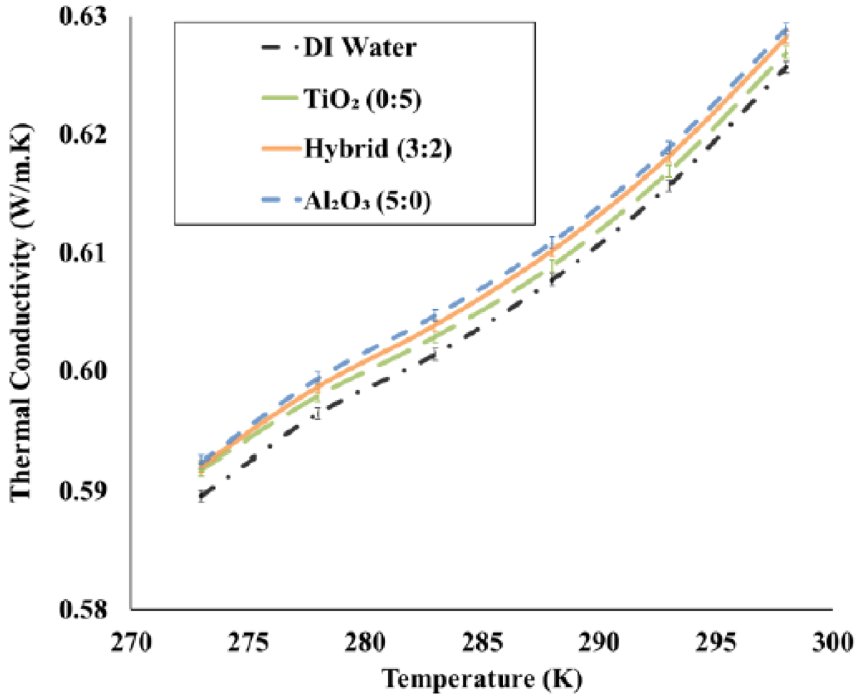

Figure 6. Thermal conductivity versus temperature for different fluids.

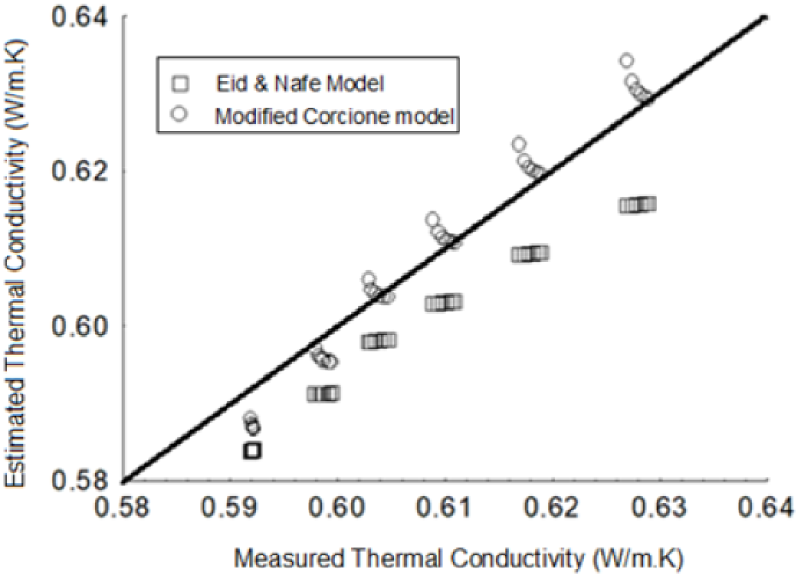

Figure 7. Comparison of measured and estimated thermal conductivity for hybrid nanofluid.

Table 5. Effective viscosity (μ_{eff}) of Al_2O_3 and TiO_2 nanofluids (0.1 v%) with temperature.

Temperature, T (K)	Effective Viscosity, μ_{eff} (mPa·s)			
	Al_2O_3 Nanofluid Model 3		TiO_2 Nanofluid	
	Test	Equation (3)	Test	Equation (3)
283	0.9684	0.9600	0.9684	0.9614
288	0.8786	0.8753	0.8935	0.8766
293	0.8187	0.8194	0.8275	0.8206
298	0.7535	0.7533	0.7690	0.7544

Table 6. Effective viscosity (μ_{eff}) of Al_2O_3 nanofluid (0.1 v%) at 323 K varying concentration (ϕ).

Concentration, ϕ	Effective Viscosity, μ_{eff} (mPa·s)	
	Test [50,53]	Equation (3)
0.005	0.5467	0.5536
0.010	0.5596	0.5706
0.015	0.5763	0.5891
0.020	0.5973	0.6089
0.025	0.6220	0.6304
0.030	0.6511	0.6536
0.035	0.6839	0.6786
0.040	0.7211	0.7058

Table 7. Effective viscosity (μ_{eff}) of hybrid nanofluid having different particle ratios at a specific temperature.

Fluid	Effective Viscosity, μ_{eff} (mPa·s)			
	Temperature, T (K)			
	283	288	293	298
DI Water	0.9549	0.8706	0.8150	0.7493
TiO_2 (0:5)	0.9707	0.8850	0.8285	0.7617
Hybrid (1:4)	0.9690	0.8835	0.8271	0.7604
Hybrid (2:3)	0.9683	0.8828	0.8264	0.7598
Hybrid (3:2)	0.9679	0.8824	0.8261	0.7595
Hybrid (4:1)	0.9675	0.8821	0.8258	0.7592
Al_2O_3 (5:0)	0.9673	0.8819	0.8256	0.7590

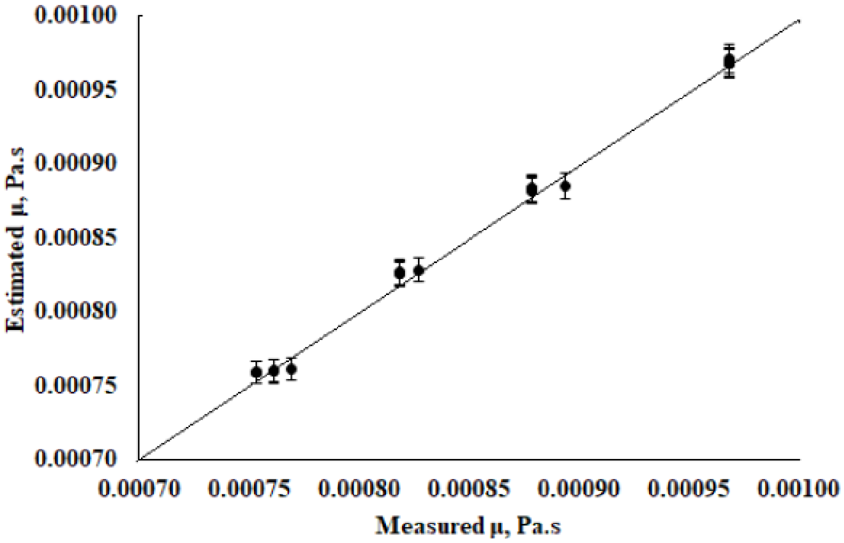

Figure 8. Estimated and measured effective viscosity, (Pa·s) of hybrid nanofluid.

Table 8. Recorded cold and hot fluids outlet temperature keeping the hot inlet temperature (T_{hi}) at 35 °C and varying the cold inlet temperature (T_{ci}).

Fluid	Outlet Temperature, T_{co} (°C) of the Cold Fluid				Outlet Temperature, T_{ho} (°C) of the Hot Fluid			
	Cold Inlet Temperature, T_{ci} (°C)				Cold Inlet Temperature, T_{ci} (°C)			
	10	15	20	25	10	15	20	25
DI water	23.55	26.20	28.85	30.95	21.42	23.81	26.44	28.95
TiO_2 (0:5)	23.65	26.32	29.06	31.15	21.40	23.72	26.39	28.91
Hybrid (1:4)	23.68	26.37	29.10	31.28	21.39	23.69	26.37	28.89
Hybrid (2:3)	23.72	26.44	29.18	31.41	21.37	23.66	26.35	28.87
Hybrid (3:2)	23.76	26.53	29.27	31.50	21.35	23.63	26.33	28.85
Hybrid (4:1)	23.79	26.61	29.35	31.59	21.33	23.60	26.31	28.83
Al_2O_3 (5:0)	23.82	26.69	29.43	31.68	21.31	23.59	26.30	28.82

Table 9. Thermo-physical properties of fluids at 25 °C.

	Cp (J/kg·K)	k (W/m·K)	ρ (kg/m^3)	μ (mPa·s)
DI water	4183	0.6077	994.7	0.7493
TiO_2 (0:5)	4169	0.6136	997.9	0.7544
Hybrid (1:4)	4169	0.6120	997.7	0.7538
Hybrid (2:3)	4169	0.6114	997.6	0.7536
Hybrid (3:2)	4169	0.6110	997.4	0.7535
Hybrid (4:1)	4169	0.6108	997.4	0.7534
Al_2O_3 (5:0)	4170	0.6107	997.3	0.7533

Table 10. Performance parameters varying coolant inlet temperature from 283 K to 298 K.

	Heat Transfer Rate, Q (kW)				Pressure Drop, Δp_c (Pa)			
	283 K	288 K	293 K	298 K	283 K	288 K	293 K	298 K
DI water	2833.983	2342.48	1790.978	1264.443	315.01	310.46	305.5	300.4
TiO_2 (0:5)	2845.343	2359.654	1810.557	1281.66	316.25	311.5	307.4	302.6
Hybrid (1:4)	2851.596	2360.077	1812.895	1286.066	316.16	311.31	307.21	302.42
Hybrid (2:3)	2859.934	2372.668	1818.571	1289.165	316	311.09	307.13	302.26
Hybrid (3:2)	2868.272	2378.429	1832.332	1295.925	315.9	310.89	306.78	302.1
Hybrid (4:1)	2869.526	2390.105	1839.008	1301.686	315.76	310.75	306.53	301.84
Al_2O_3 (5:0)	2870.779	2407.365	1848.155	1307.78	315.64	310.64	306.38	301.61
	Nusselt number, Nu_{nf}				Prandtl number, Pr_{nf}			
DI water	10.116	11.056	12.274	14.353	6775	6106	5645	5143
TiO_2 (0:5)	10.192	11.351	12.683	14.997	6821	6158	5715	5262
Hybrid (1:4)	10.248	11.400	12.767	15.112	6819	6116	5669	5244
Hybrid (2:3)	10.333	11.597	12.984	15.368	6819	6115	5665	5225
Hybrid (3:2)	10.418	11.763	13.350	15.760	6818	6114	5661	5204
Hybrid (4:1)	10.455	11.969	13.620	16.169	6817	6113	5658	5182
Al_2O_3 (5:0)	10.484	12.209	13.898	16.713	6817	6111	5656	5158
	Heat transfer coefficient, α_{nf} (W/m^2.K)				Performance Index, PI			
DI water	1217.26	1345.69	1506.43	1780.02	549.49	454.39	347.58	245.51
TiO_2 (0:5)	1231.13	1385.00	1562.34	1864.27	551.72	457.67	351.31	248.80
Hybrid (1:4)	1238.34	1394.31	1575.24	1881.25	552.84	457.76	351.77	249.66
Hybrid (2:3)	1248.58	1418.40	1602.10	1913.42	554.47	460.22	352.88	250.27
Hybrid (3:2)	1258.94	1438.95	1647.46	1964.82	556.09	461.34	355.56	251.58
Hybrid (4:1)	1263.59	1464.10	1680.88	2015.89	556.34	463.61	356.86	252.71
Al_2O_3 (5:0)	1267.07	1493.51	1715.09	2083.64	556.59	466.97	358.64	253.90

6. Conclusions

The efficiency of a plate-type heat exchanger (PHE) hinges largely on key thermal properties, particularly thermal conductivity. To augment thermal conductivity, nanoparticles are introduced into the base fluid. This research endeavors to introduce empirical models aimed at discerning the thermal conductivity and viscosity of TiO2-Al2O3/water hybrid nanofluids. The models are tailored by adjusting the Corcione empirical relations with experimentally acquired data. These models are designed to provide estimations of both binary and mono nanofluids' thermal conductivity and viscosity. In essence, this study seeks to develop predictive tools that can accurately gauge the thermal properties of TiO2-Al2O3/water hybrid nanofluids. These tools are valuable for optimizing the performance of plate-type heat exchangers, as they allow for a better understanding of how these nanofluids influence heat transfer efficiency in such systems.

References

[1] Rostami, S.; Shahsavar, A.; Kefayati, G.; Shahsavar Goldanlou, A. Energy and Exergy Analysis of Using urbulator in a Parabolic Trough Solar Collector Filled with Mesoporous Silica Modified with Copper Nanoparticles Hybrid Nanofluid. Energies 2020, 13,2946. [CrossRef]

[2] Yadav, Y. P., & Tiwari, G. N. (1989). Demonstration plants of fibre reinforced plastic multiwick solar still: an experimental study. Solar & wind technology, 6(6), 653-666.

[3] Saba, S. S., Sreelakshmi, D., Kumar, P. S., Kumar, K. S., & Saba, S. R. (2020). Logistic regression machine learning algorithm on MRI brain image for fast and accurate diagnosis. International Journal of Scientific and Technology Research, 9(3), 7076-7081.